

# Thermal Collapse of a Skyrmion

Amel Derras-Chouk,<sup>1</sup> Eugene M. Chudnovsky,<sup>1</sup> and Dmitry A. Garanin<sup>1</sup>

*Physics Department, Herbert H. Lehman College and Graduate School, The City University of New York  
250 Bedford Park Boulevard West, Bronx, New York 10468-1589, USA*

(Dated: 15 July 2019)

Thermal collapse of an isolated skyrmion on a two-dimensional spin lattice has been investigated. The method is based upon solution of the system of stochastic Landau-Lifshitz equations for up to  $10^4$  spins. The recently developed pulse-noise algorithm has been used for the stochastic component of the equations. The collapse rate follows the Arrhenius law. Analytical formulas derived within a continuous spin-field model support numerically-obtained values of the energy barrier. The pre-exponential factor is independent of the phenomenological damping constant that implies that the skyrmion is overcoming the energy barrier due to the energy exchange with the rest of the spin system. Our findings agree with experiments, as well as with recent numerical results obtained by other methods.

## I. INTRODUCTION

Skyrmions are whirls of spins stabilized by topology. The topological protection of skyrmions has motivated recent research on their nucleation and manipulation in thin magnetic films. It arises from the mapping of a three-component fixed-length spin field on a two-dimensional (2D) coordinate space<sup>1-3</sup>. The topologically protected metastable skyrmions solutions for the 2D Heisenberg exchange model in the continuous approximation obtained by Belavin and Polyakov (BP)<sup>4</sup> are scale invariant, that is, their energy is independent of their size. In practice, scale invariance is violated by the discreteness of the atomic lattice<sup>5</sup>, as well as by other interactions such as Zeeman interaction, dipole-dipole interaction (DDI), perpendicular magnetic anisotropy (PMA), interaction of skyrmions with defects and boundaries, etc. This leads to the stabilization of the skyrmion size at some value minimizing the total energy, or, to the contrary, to their collapse or expansion followed by the transformation into the domain structure.

Currently, there is a great interest in skyrmions in non-centrosymmetric materials. The lack of inversion symmetry results in the Dzyaloshinskii-Moriya interaction (DMI). It competes with other material-dependent interactions, providing metastability or even thermodynamic stability of skyrmions within a certain area of the phase diagram<sup>6,7</sup>. Stable isolated skyrmions have been experimentally observed<sup>8-10</sup> even at room temperatures.

Skyrmions provide a promising avenue for new forms of memory storage because information can be encoded in them as bits<sup>6,10-15</sup>. Recent advances in nucleation methods have accelerated interest in skyrmions by demonstrating the feasibility of skyrmion writing devices. One promising method involves application of a spin-polarized current using a scanning tunneling microscope. Such a method can both nucleate and erase skyrmions, as was demonstrated on a PbFe/Ir(111) system<sup>22</sup>. Additionally, recent experimental and theoretical work has explored the possibility of skyrmion creation by temperature<sup>17</sup>, by local heating<sup>18,19</sup> and with the help of the magnetic force microscope (MFM) tip<sup>20</sup> or of a magnetic dipole<sup>21</sup>. The existence of skyrmions depends on both the material parameters and the external conditions, such as the magnetic field and temperature. It has been experimentally

demonstrated that the size of a skyrmion can be tuned by the external field, with its radius shrinking on increasing the field opposite to the direction of spins in the skyrmion until the skyrmion disappears<sup>22,23</sup>.

The longevity of metastable skyrmions with respect to thermal or quantum collapse (also called thermal or quantum stability) is important for potential applications. Quantum decay of a skyrmion has been recently studied by a method based upon finding an instanton solution of the imaginary-time equations of motion<sup>24</sup>. The statistical mechanics problem of the thermal collapse of a skyrmion is more involved. It has been explored for various systems, both for a skyrmion in a racetrack<sup>25,26</sup> and an isolated skyrmion in a thin film<sup>27-31</sup>. Although most of the investigators have studied purely 2D systems<sup>25,26,28-30,32,33</sup>, some have considered multilayered systems as well<sup>27</sup>. The latter are relevant to recent experimental advances in creating room temperature skyrmions, while numerical models of purely 2D systems apply to skyrmions found in B20 materials<sup>34</sup>. Some previous work uses Monte Carlo simulations<sup>29,31,33</sup> that capture the main physics of the thermally-activated decay but cannot establish its overall time scale for the lack of connection to the actual dynamics. There are semi-analytical methods that search for the minimum-energy path out of the metastable state to find the energy barrier<sup>25-28,30,32,35</sup>. One of these methods is the Nudged Elastic Band Method (NEBM)<sup>25-28,32,35</sup>, that is efficient in the cases when the decay path is not obvious since it is mediated by the proximity of the skyrmion to the defects or to the boundaries. After the decay path is found, the skyrmion decay rate is usually written in the form of the Arrhenius expression with the exponent defined by the energy barrier and the prefactor given by the Langer's formula<sup>28</sup>.

In this paper, we present the results of the lifetime computations for an isolated metastable skyrmion using the Landau-Lifshitz equation<sup>36</sup> for a system of classical spins augmented by the stochastic Langevin fields, the so-called Landau-Lifshitz-Langevin (LLL) equation. In comparison to the Monte Carlo simulations, this method is more realistic as it describes the actual dynamics of the system. We consider skyrmions in an pure infinite 2D system, modeled by a finite system with periodic boundary conditions. In this case, one can estimate the energy barrier analytically to compare with the numerical results without a need to use NEMB and similar involved numerical methods.

For a single spin, as well as for a single particle, the prefactor in the Arrhenius escape rate nontrivially depends on the damping constant that accounts for the coupling with the bath, considered phenomenologically. There are regimes of high, intermediate, and weak damping, first found by Kramers<sup>37</sup> for the particle and later established for the spin by Brown<sup>38</sup> and later workers (see, e.g., Refs.<sup>40,41</sup>). The stochastic equation of motion for the particle or spin is equivalent to the corresponding Fokker-Planck equation that can be solved analytically or numerically. In particular, at low temperatures the decay rate is controlled by the lowest eigenvalue of the Fokker-Planck operator.

The situation is different for many-body systems such as spin systems with skyrmions. First, the multidimensional Fokker-Planck equation cannot be solved numerically (although the analytical Langer's approach is still possible under the assumption of a high-to-intermediate damping<sup>28</sup>). Thus the direct solution of the LLL equation for a system of spins is the only available numerical method, quite feasible with the modern computing power (for a recent reference, see Ref.<sup>42</sup>). Second, the skyrmion can exchange its energy with the rest of the spin system, in particular, with the reservoir of spin waves. The thermal energy of the system is proportional to its size and exceeds by far the energy needed for a skyrmion to overcome the barrier and collapse. Thus, it is not obvious whether the phenomenological bath is playing any role in the dynamics in the realistic low-damping case, apart from providing the temperature to the systems via the balance of excitation and damping. Indeed, our results show that the prefactor in the skyrmion collapse rate is independent of the damping constant  $\alpha$ , the so-called Gilbert constant.

In this paper, the LLL equation is treated with the help of the recently developed pulse-noise approach<sup>43,44</sup> that replaces the continuous white noise by discrete noise pulses between which the dynamics of the spin system can be computed by a standard high-order ordinary-differential-equation (ODE) solvers. This approach works well in the case of low damping typical for spin systems, and it reproduces the results of the LLL equation solved by standard methods, however, with the computational speed of the noiseless dynamics. At low temperatures, the results fit the Arrhenius law, typical for overbarrier transitions driven by temperature<sup>25–28,30,32,35</sup>. Indeed, the Arrhenius law has been observed experimentally in the decay of the array of skyrmions in a film<sup>45</sup>.

The paper is organized as follows. In Section II the analytical model of the static properties of the skyrmion based on the BP skyrmion shape is discussed. In Section III, the dynamics is introduced and the numerical method are presented. In Section IV, results of the numerical computation and comparison to the analytical model are given. Lastly, a discussion of the results is done in Section V.

## II. THE MODEL

We consider a two-dimensional square lattice of spins considered as normalized three-component vectors,  $\mathbf{s}_i \equiv \mathbf{S}_i/S$ , where  $S$  is the atomic spin value and  $i$  refers to the lattice site.

The Hamiltonian of the system is given by

$$\begin{aligned} \mathcal{H} = & -\frac{S^2}{2} \sum_{ij} J_{ij} \mathbf{s}_i \cdot \mathbf{s}_j \\ & - S^2 A \sum_i (\mathbf{s}_i \times \mathbf{s}_{i+\hat{x}}) \cdot \hat{x} + (\mathbf{s}_i \times \mathbf{s}_{i+\hat{y}}) \cdot \hat{y} \\ & - \mathbf{S}\mathbf{H} \cdot \sum_i \mathbf{s}_i. \end{aligned} \quad (1)$$

The first term represents the Heisenberg exchange energy with the exchange constant  $J$  between the nearest neighbors. The second term represents the Dzyaloshinskii-Moriya interaction (DMI). For certainty we have chosen a Bloch type DMI that favors the Bloch-type skyrmions with the chirality angle  $\gamma = \pi/2$  (see below) for  $A > 0$ . The last term is the Zeeman interaction energy due to the external magnetic field induction  $\mathbf{B}$ , and  $\mathbf{H} \equiv g\mu_B\mathbf{B}$  is the magnetic field in the energy units (with  $\mu_B$  being the Bohr magneton and  $g$  being the gyromagnetic factor). The skyrmion that we consider will be stabilized by a field applied perpendicular to the plane so that the Zeeman term becomes  $-SH \sum_i s_{i,z}$ .

The continuous analog of this energy is

$$\begin{aligned} \mathcal{H} = & \frac{1}{2} JS^2 \int dx dy \left[ \left( \frac{\partial \mathbf{s}}{\partial x} \right)^2 + \left( \frac{\partial \mathbf{s}}{\partial y} \right)^2 \right] \\ & - \frac{1}{24} JS^2 \int dx dy \left[ \left( \frac{\partial^2 \mathbf{s}}{\partial x^2} \right)^2 + \left( \frac{\partial^2 \mathbf{s}}{\partial y^2} \right)^2 \right] \\ & + AS^2 \int dx dy \left[ \left( \mathbf{s} \times \frac{\partial \mathbf{s}}{\partial x} \right) \cdot \hat{x} + \left( \mathbf{s} \times \frac{\partial \mathbf{s}}{\partial y} \right) \cdot \hat{y} \right] \\ & - HS \int dx dy s_z, \end{aligned} \quad (2)$$

where all lengths are measured in the units of the lattice spacing  $a$ . The second term in this expression arises from taking into account the next derivatives in the expansion of the discrete form of the exchange energy that becomes important for small-size skyrmions creating large gradients of the spin field.

The continuous unit-length spin field  $\mathbf{s}$  is characterized by the topological charge:

$$Q = \frac{1}{4\pi} \int dx dy \mathbf{s} \cdot \left( \frac{\partial \mathbf{s}}{\partial x} \times \frac{\partial \mathbf{s}}{\partial y} \right). \quad (3)$$

that takes discrete values  $Q = 0, \pm 1, \pm 2, \dots$

The first, dominant, term in Eq. (2) gives rise to the Belavin-Polyakov (BP) skyrmion<sup>4</sup> with the spin components

$$\begin{aligned} s_x &= 2\lambda \frac{r(\cos \phi \cos \gamma - \sin \phi \sin \gamma)}{r^2 + \lambda^2}, \\ s_y &= 2\lambda \frac{r(\sin \phi \cos \gamma + \cos \phi \sin \gamma)}{r^2 + \lambda^2}, \\ s_z &= \frac{\lambda^2 - r^2}{\lambda^2 + r^2} \end{aligned} \quad (4)$$

written as functions of polar coordinates,  $r = \sqrt{x^2 + y^2}$  and  $\phi$ , in the  $xy$  plane. Here  $\lambda$  is the skyrmion size and  $\gamma$  is the chirality angle. It is the energy minimum of the first term in Eq.

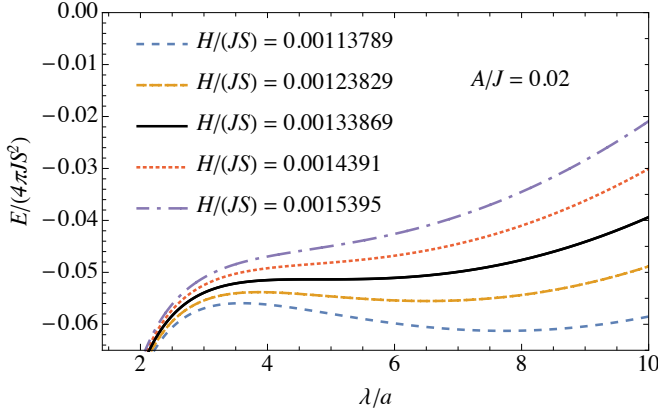


FIG. 1. Energy vs size for an isolated metastable skyrmion at various fields. The skyrmion size  $T = 0$  corresponds to the metastable energy minimum. As the field increases, the minimum eventually disappears and the skyrmion becomes absolutely unstable against the collapse.

(2) within the homotopy class  $Q = 1$ . That energy minimum is independent of  $\lambda$  and  $\gamma$  and equals  $E = 4\pi JS^2$ .

Interactions weaker than the ferromagnetic exchange that are present in Eqs. (1) and (2) deform the BP skyrmion and make its energy depend on  $\lambda$  and  $\gamma$ . However, for the smallest skyrmions the extremal solution of the corresponding equations of motion are still close to the BP shape<sup>24</sup>. This allows one to evaluate the energy of a small skyrmion by substituting Eq. (4) into Eq. (2). The result reads

$$E = 4\pi JS^2 - \frac{2\pi JS^2}{3\lambda^2} - 4\pi AS^2\lambda \sin \gamma + 4\pi |H| S \lambda^2 I(\lambda). \quad (5)$$

The second term in Eq. (5) comes from the discreteness of the lattice. It favors the shrinkage of the skyrmion<sup>5</sup>. The third and the fourth terms come from the integration of the DMI and Zeeman interactions. The factor  $I(\lambda)$  depends logarithmically on  $\delta_H/\lambda$  and  $L/\lambda$ , with a shorter of the two lengths,  $\delta_H = \sqrt{JS/|H|}$  or the size of the system  $L$ , dominating the dependence. For  $\lambda \ll \delta_H$  a more accurate expression is given by<sup>24</sup>

$$I(\lambda) = \ln(1.5 + 0.68\delta_H/\lambda) \quad (6)$$

that will be used below. Stabilizing magnetic field is applied opposite to the magnetic moment of the skyrmion, making the sign of the Zeeman term positive.

The energy in Eq. (5) is minimized by the Bloch-type skyrmion with  $\gamma = \pi/2$  for  $A > 0$ . It is plotted in Fig. 1, for different fields, as function of the skyrmion size  $\lambda$ . On increasing the field the energy minimum shifts towards smaller  $\lambda$ . At  $|H| > H_c$  the minimum no longer exists, making skyrmions of size  $\lambda < \lambda_{\text{crit}}$  absolutely unstable against the collapse.

With the logarithmic accuracy  $|\lambda_{\text{crit}}|/(JS) \sim (A/J)^{4/3}$  and  $\lambda_{\text{crit}}/a \sim (J/A)^{1/3}$ . Close to the critical field the energy barrier in Eq. (5) scales as

$$\frac{U}{JS^2} \propto \left(\frac{A}{J}\right)^{2/3} \left(1 - \frac{|H|}{H_{\text{crit}}}\right)^n, \quad n = \frac{3}{2}. \quad (7)$$

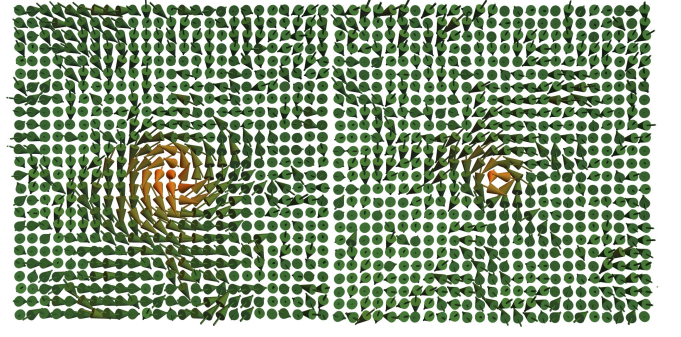


FIG. 2. Stages of skyrmion thermal collapse. From left to right: The skyrmion shrinks while preserving its Bloch shape with the counter-clockwise rotation. Color code: green/orange = negative/positive  $s_z$ .

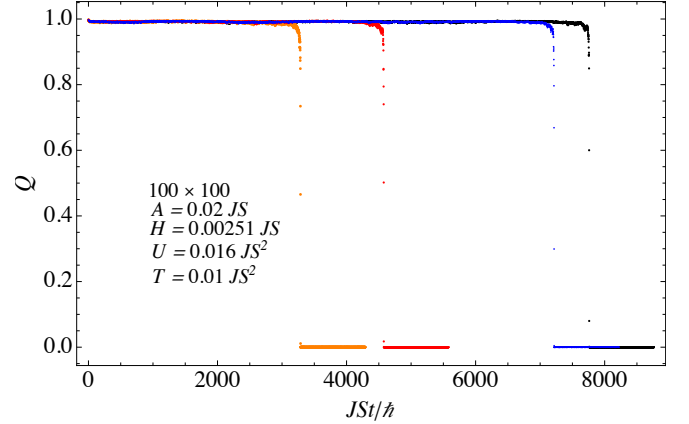


FIG. 3. Different events of skyrmion collapse detected by the time dependence of the topological charge  $Q(t)$ .

### III. DYNAMICS AND NUMERICAL METHODS

We approach the problem of skyrmion thermal collapse by solving the LLL equation on a 2D lattice. The time evolution of each spin on the lattice satisfies<sup>1,36,38</sup>

$$\dot{\mathbf{s}}_i = \gamma[\mathbf{s}_i \times (\mathbf{B}_{\text{eff},i} + \boldsymbol{\zeta}_i)] - \gamma\alpha[\mathbf{s}_i \times (\mathbf{s}_i \times \mathbf{B}_{\text{eff},i})], \quad (8)$$

where  $\gamma = g\mu_B/\hbar$  is the gyromagnetic ratio,  $\alpha$  is a dimensionless damping constant,  $\mathbf{B}_{\text{eff},i}$  is the effective magnetic field induction acting in the  $i$ -th spin and given by  $\mu_0\mathbf{B}_{\text{eff},i} = -\partial\mathcal{H}/\partial\mathbf{s}_i$ ,  $\mu_0 = g\mu_B S$  is the magnetic moment associated with  $\mathbf{s}_i$ , and  $\boldsymbol{\zeta}_i$  is the stochastic field due to thermal fluctuations. The equilibrium solution of Fokker-Planck equation corresponding to this stochastic differential equation should be the Boltzmann distribution, which requires that the stochastic field components satisfy the white-noise condition

$$\langle \zeta_{\nu,i}(t), \zeta_{\beta,j}(t') \rangle = \frac{2\alpha k_B T}{\gamma\mu_0} \delta_{ij} \delta_{\nu\beta} \delta(t-t'), \quad (9)$$

where  $T$  is the temperature.

To speed up the numerical integration of the LLL equation, one can replace the continuous white noise by the pulse noise

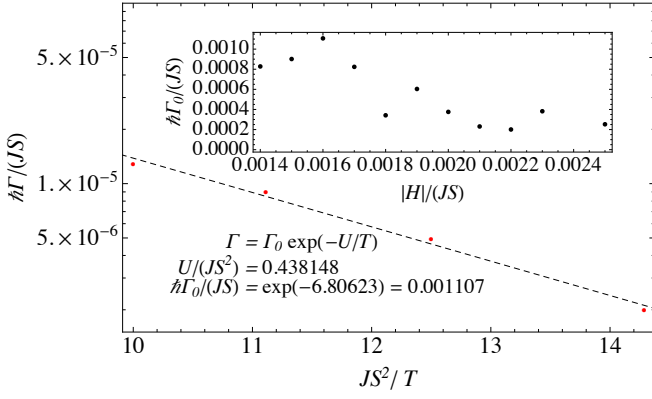


FIG. 4. Arrhenius dependence of the collapse rate  $\Gamma$  on temperature at  $|H|/(JS) = 0.0016$ . Inset: Pre-exponential factor in the Arrhenius law for the collapse rate law at various magnetic fields.

with the period  $\Delta t$ <sup>43,44</sup>. Noiseless evolution during the interval  $\Delta t$  between the pulses can be computed by an efficient high-order ODE solver such as fourth-order Runge-Kutta method with the integration step  $\delta t \ll \Delta t$  for weak damping.

Noise pulses rotate each spin by the angle

$$\phi_i = \sqrt{\Lambda_N \Delta t} \mathbf{G}_i, \quad (10)$$

where

$$\Lambda_N \equiv \frac{2\gamma\alpha k_B T}{\mu_0} = \frac{2\alpha k_B T}{\hbar S} \quad (11)$$

is the so-called Néel attempt frequency and  $\mathbf{G}_i$  is a three-component vector, each component being a realization of a normal distribution with dispersion  $\sigma = 1$ , so that  $\langle G_{i\alpha} G_{j\beta} \rangle = \delta_{ij} \delta_{\alpha\beta}$ . With  $\boldsymbol{\varphi} = \boldsymbol{\varphi}_n$  and  $|\mathbf{n}| = 1$  the spin rotation formula reads

$$\mathbf{s}' = \mathbf{s} \cos \varphi + (\mathbf{n} \times \mathbf{s}) \sin \varphi + \mathbf{n} (\mathbf{s} \cdot \mathbf{n}) (1 - \cos \varphi). \quad (12)$$

The applicability of the pulse-noise model requires that both random rotation angles and the non-thermal relaxation angles during the interval  $\Delta t$  between the pulses be small:

$$\phi \sim \sqrt{\Lambda_N \Delta t} \ll 1, \quad \gamma\alpha B_{\text{eff}} \Delta t \ll 1. \quad (13)$$

These conditions set an upper limit on  $\Delta t$ . However, for  $\alpha \ll 1$  and low temperatures,  $\Delta t$  can be much larger than the noiseless integration step  $\delta t$  that is, in turn, limited by the exchange interaction, as the stability of typical ODE solvers requires  $\delta t \lesssim 0.2\hbar/(JS)$ . For  $\delta t \ll \Delta t$  most of the computer time is spent on computing the noiseless evolution, whereas random spin rotations take negligible computer time. Testing of different choices for  $\Delta t$  and  $\delta t$  for a many-spin system can be found in Sec. IV of Ref.<sup>43</sup>. Those who wish to implement the pulse-noise routine, can test it at equilibrium comparing to Monte Carlo.

Our computations were done on a  $100 \times 100$  lattice with periodic boundary conditions. The temperature is measured

in the energy units,  $k_B \Rightarrow 1$ . All energies have been measured in units of  $JS^2 = 1$ , while times have been measured in units of  $\hbar/(JS)$ . The DMI constant  $A$  was set to  $0.02J$ . The noise-free time interval  $\Delta t = 2$  and the noise-free integration step  $\delta t = 0.2$  with the fourth-order Runge-Kutta method were used. Most of the computations were performed with the damping parameter  $\alpha = 0.01$ , so the conditions in Eq. (13) were satisfied.

First, the metastable energy minimum for the skyrmion was found by the energy minimization at  $T = 0$ . This computation also yields the numerical value of the critical field for the skyrmion collapse,  $H_{\text{crit},N}$ . Then, the thermal noise was switched on and the LLL was solved until the maximum time of  $t_{\text{max}} = 10^6$ . Such computations were run in parallel 300 times for each set of parameters on a 40-node computing cluster. The skyrmion collapse was detected by the change of the topological charge  $Q$  from the value close to 1 to the value close to zero (thermal fluctuations wash out the value of  $Q$  only slightly). We used the four-point lattice approximation for the first derivatives in the formula for  $Q$ , Eq. (3). After the skyrmion collapse or after reaching the maximal time, the particular computation was terminated and a new one began. The collected statistics of collapse times was used to extract the collapse rate  $\Gamma$  with the help of the new algorithm that does not require that all skyrmions collapse (see the Appendix of Ref.<sup>44</sup>). Finally, the obtained data for  $\Gamma$  were fit to the Arrhenius law,  $\Gamma = \Gamma_0 \exp(-U/T)$ , to extract the exponent  $U$  and the prefactor  $\Gamma_0$ .

#### IV. NUMERICAL RESULTS AND ANALYSIS

Snapshots of spin configurations at an elevated temperature in Fig. 2 show a significant thermal disordering of spins and deformation of the skyrmion seen in the middle. In spite of this, detection of the skyrmion by the topological charge  $Q$  is quite reliable. A sample of time dependences  $Q(t)$  showing the skyrmion collapse is given in Fig. 3.

The extracted dependence of the skyrmion collapse rate  $\Gamma$  on temperature together with the magnetic-field dependence of the prefactor  $\Gamma_0$  is shown in Fig. 4. The former is a straight line in the Arrhenius plot that confirms the expected Arrhenius dependence  $\Gamma = \Gamma_0 \exp(-U/T)$ . The prefactor  $\Gamma_0$  in the inset decreases with increasing  $|H|$ . Whereas there is no comprehensive theory yet, one can expect that the skyrmion is relaxing by the energy exchange with spin waves. Increasing  $|H|$  pushes the gap in the spin-wave spectrum up, whereas the frequency of the skyrmion oscillations near its energy minimum decreases as the minimum flattens. Thus, the frequency mismatch between the skyrmion and spin waves increases that suppresses the energy exchange between them.

Table I shows the values of the barrier and the prefactor for different values of  $\alpha$  computed for  $|H|/(JS) = 0.0019$ . Whereas the same values of  $U$  are natural and only provide a self-consistency check of our computations, the absence of the  $\alpha$ -dependence of the prefactor (within the numerical accuracy of the computations) indicates the dominance of the intrinsic damping mechanism in our system.

$\alpha$	0.01	0.02	0.04	0.06	0.08	0.1
$U/(JS^2)$	0.235	0.216	0.223	0.210	0.175	0.210
$\hbar\Gamma_0/(JS) \times 10^3$	0.604	0.687	1.03	1.04	0.760	1.36

TABLE I. The energy barrier  $U$  and prefactor  $\Gamma_0$  of the skyrmion collapse are independent of the damping constant  $\alpha$  within the numerical accuracy (data for  $|H|/(JS) = 0.0019$ ).

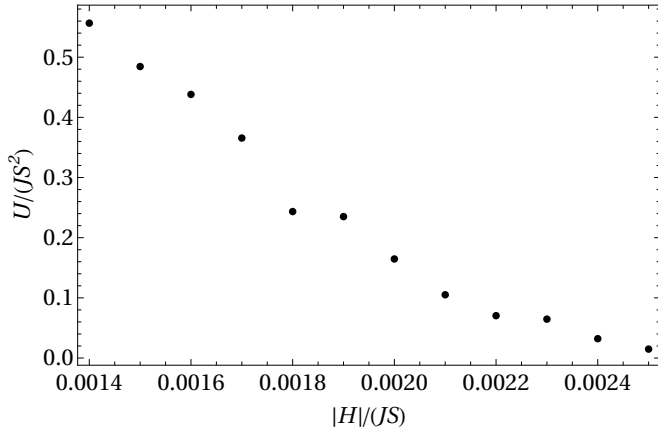


FIG. 5. Energy barrier for the skyrmion collapse  $U$  vs the external magnetic field  $|H|$ .

The energy barriers obtained from the Arrhenius law at various magnetic fields are presented in Fig. 5. It is interesting to compare the values determined numerically to the ones found by computing the difference between the maximum and minimum of the energy curve in Eq. (5). Notice that the analytical model assumes quasi-continuity of the spin-field. Consequently, the results obtained analytically for the continuous spin field and numerically with the discrete model are expected to be close to each other only when spins rotate by a small angle from one lattice site to the neighboring one. This is certainly not the case for small skyrmions, see Fig. 2. Nevertheless, a qualitative agreement should be expected. While one cannot directly compare values at the same external field in both models, comparison of the barriers at the same displacement from the critical field offers some interesting agreement. The critical field in the discrete numerical model is  $H_{\text{crit,N}} = 0.00259JS$ , while the one in the analytical model (determined by the inflection point in the energy vs  $\lambda$  in Fig. 1) is  $H_{\text{crit,A}} = 0.00134JS$ . Away from the critical field, we show that the barriers obtained by the two methods are approximately the same when computed as functions of  $1 - |H|/H_{\text{crit}}$ , see Fig. 6.

The typical values of the pre-exponential factor in the Arrhenius law in problems of thermal collapse range from  $10^9$  to  $10^{11}$  Hz, as found by spin dynamics computations<sup>30,31</sup>. Our results shown in the inset of Fig. 4 are in accordance with this after conversion to natural units. Using the typical value  $J = 10^3$  K and  $S = 1$ , one obtains the values of the order from  $10^9$  to  $10^{11}$  Hz for  $\Gamma_0$  in Fig. 4. The magnetic-field dependence of the prefactor is similar to that observed in the experiment<sup>45</sup>.

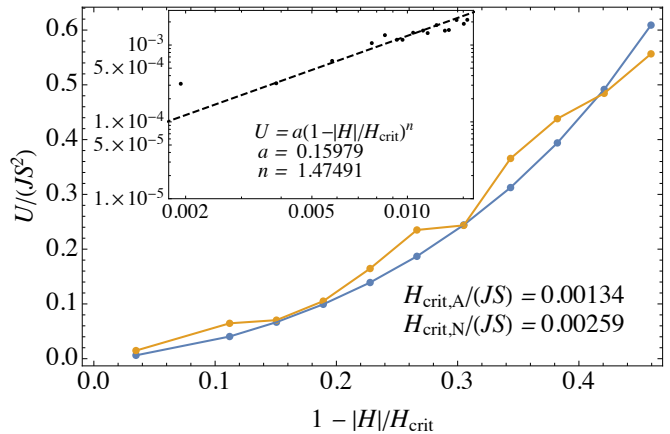


FIG. 6. Field dependence of the energy barrier for numerical (orange) and analytical (blue) models compared for the same displacements from their respective critical fields. The barrier dependence of the analytical model has been calculated from Eq. (5). Inset: Numerically found dependence of the energy barrier on the deviation of the magnetic field from the critical point (log-log scale).

A temperature-dependent analysis of the prefactor has been given in Ref.<sup>26</sup> in which the authors used the presence of Goldstone modes to derive the influence of the temperature. However, our numerical results do not show any dependence of the prefactor on the temperature and phenomenological damping.

Having derived in Section II the analytical relationship between the energy barrier and the small deviation from the critical field, Eq. (7), we can compare it with our numerical results. Fitting to Eq. (7) yields  $n = 1.47$  that is close to the analytical value  $n = 3/2$ . This result is interesting because of the  $3/2$  power-law dependence of the energy barrier has been observed in resonant tunneling structures<sup>46,47</sup>.

## V. DISCUSSION

The values used in the computations were  $S = 1$  for the spin,  $A/J = 0.02$  for the ratio of DMI to exchange, and  $\alpha = 0.01$  for the damping parameter. The value of the exchange constant  $J = 10^3$  K was chosen for estimates of the Arrhenius prefactor. These are typical parameters of magnetic materials used in the experiments with skyrmions.

With the parameters chosen, the energy barriers for the skyrmion collapse ranged from a few meV to a few tens of meV depending on the field. Such a strong dependence of the energy barrier on the magnetic field in the same ball park has been observed experimentally in a skyrmion lattice<sup>45</sup>.

The previous work has suggested that the skyrmion collapse rate may be affected by changes in the pre-exponential factor alongside with the changes in the energy barrier<sup>26,45</sup>. We found evidence of this effect on our simulations. This motivates further research on how the pre-exponential factor impacts the skyrmion lifetime at elevated temperatures.

Since we considered a system with periodic boundary conditions, the only way for the skyrmion to vanish (besides

quantum decay<sup>24</sup> was its spontaneous over-barrier shrinking due to thermal fluctuations to the size below which it collapses. This is a generic problem of skyrmion thermal collapse that must be of interest for experiments with skyrmions at elevated temperatures, as well as for applications of skyrmions in logic devices.

It has been shown previously<sup>26</sup> that in systems with boundaries there is a range of external fields for which skyrmion escape through the boundary has a lower energy barrier than that for the internal collapse. This possibility has sparked interest in methods of suppressing such escape by, e.g., altering the DMI at the boundary<sup>27</sup>. It has been shown that skyrmion stability can also be increased by the exchange frustration<sup>35</sup>. Our method can be easily generalized for the study of these effects as well as for the studies of bilayers<sup>34</sup> and slabs.

## VI. CONCLUSION

We have numerically modeled the thermal collapse of a skyrmion stabilized by the ferromagnetic exchange, DMI, and external magnetic field in a two-dimensional lattice. Using the stochastic Landau-Lifshitz equation and approximating thermal fluctuations through a pulse-noise model, we have computed the time evolution of each spin in the lattice. In this way, we modeled the evolution of the skyrmion in time. We used these results to calculate the energy barrier of a skyrmion, and confirmed them with an analytical model. Additionally, order of magnitude agreement of energy barriers with experiment indicate that modelling the real time dynamics of skyrmions using the pulse-noise method is an effective way of modeling skyrmions.

## VII. ACKNOWLEDGEMENTS

This work has been supported by the grant No. DEFG02-93ER45487 funded by the U.S. Department of Energy, Office of Science.

<sup>1</sup>E. M. Chudnovsky and J. Tejada, *Lectures on Magnetism*, Rinton Press (Princeton - NJ, 2006).

<sup>2</sup>Book: *The Multifaceted Skyrmion*, edited by G. E. Brown and M. Rho (World Scientific, 2010).

<sup>3</sup>N. Manton and P. Sutcliffe, *Topological Solitons*, Cambridge University Press 2004.

<sup>4</sup>A. A. Belavin and A. M. Polyakov, Pis'ma Zh. Eksp. Teor. Fiz **22**, 503-506 (1975) [JETP Lett. **22**, 245-248 (1975)].

<sup>5</sup>L. Cai, E. M. Chudnovsky, and D. A. Garanin, Phys. Rev. B **86**, 024429 (2012).

<sup>6</sup>A. O. Leonov, T. L. Monchesky, N. Romming, A. Kubetzka, A. N. Bogdanov, and R. Wiesendanger, New Journal of Physics **18**, 065003-(16) (2016).

<sup>7</sup>F. Büttner, I. Lemesh, and G. S. D. Beach, Sci. Rep. **8**, 4464 (2018).

<sup>8</sup>O. Boulle, J. Vogel, H. Yang, S. Pizzini, D. S. de Souza Chaves, A. Locatelli, T. O. Mentès, A. Sala, L. D. Buda-Prejbeanu, O. Klein, M. Belmeguenai, Y. Roussigné, Y. A. Stashkevich, S. M. Chérif, L. Aballe, M. Foerster, M. Chshiev, S. Auffret, I. M. Miron, and G. Gaudin, Nature Nanotech. **11**, 449 (2016).

<sup>9</sup>C. Moreau-Luchaire, C. Moutas, N. Reyren, J. Sampaio, C. A. F. Vaz, N. Van Horne, K. Bouzehouane, C. Garcia, K. Deranlot, P. Warnicke, P.

Wohlhüter, J.-M. George, M. Weigand, J. Raabe, V. Cros, and A. Fert, Nature Nanotech. **11**, 444 (2016).

<sup>10</sup>A. Fert, N. Reyren, and V. Cros, Nature Reviews Materials **2**, 17031-(15) (2017).

<sup>11</sup>N. Nagaosa and Y. Tokura, Nature Nanotechnology **8**, 899-911 (2013).

<sup>12</sup>R. Tomasello, E. Martinez, R. Zivieri, L. Torres, M. Carpentieri, and G. Finocchio, Nature Scientific Reports **4**, 6784-(7) (2014).

<sup>13</sup>X. Zhang, M. Ezawa, and Y. Zhou, Scientific Reports **5**, 9400-(8) (2015).

<sup>14</sup>G. Finocchio, F. Büttner, R. Tomasello, M. Carpentieri, and M. Klau, Journal of Physics D: Applied Physics. **49**, 423001-(17) (2016).

<sup>15</sup>W. Jiang, G. Chen, K. Liu, J. Zang, S. G. E. te Velthuis, and A. Hoffmann, Physics Reports **704**, 1 - 49 (2017).

<sup>16</sup>N. Romming, C. Hanneken, M. Menzel, J. E. Bickel, B. Wolter, K. von Bergmann, A. Kubetzka, and R. Wiesendanger, Science **341**, 636 (2013).

<sup>17</sup>S. Zhang, J. Zhang, Y. Wen, E. M. Chudnovsky, and X. X. Zhang, Applied Physics Letters **113**, 192403-(5) (2018).

<sup>18</sup>W. Koshibae and N. Nagaosa, Nat. Commun. **5**, 5148 (2014).

<sup>19</sup>G. Berruto, I. Madan, Y. Murooka, G. M. Vanacore, E. Pomarico, J. Rajeswari, R. Lamb, P. Huang, A. J. Kruchkov, Y. Togawa, T. LaGrange, D. McGrouther, H. M. Ronnow, and F. Carbone, Physical Review Letters **120**, 117201-(6) (2018).

<sup>20</sup>S. Zhang, J. Zhang, Q. Zhang, C. Barton, V. Neu, Y. Zhao, Z. Hou, Y. Wen, C. Gong, O. Kazakova, W. Wang, Y. Peng, D. A. Garanin, E. M. Chudnovsky, and X. X. Zhang, Applied Physics Letters **112**, 132405-(5) (2018).

<sup>21</sup>D. A. Garanin, D. Capic, S. Zhang, X. Zhang, and E. M. Chudnovsky, J. Appl. Phys. **124**, 113901 (2018).

<sup>22</sup>N. Romming, C. Hanneken, M. Menzel, J. E. Bickel, B. Wolter, K. von Bergmann, A. Kubetzka, and R. Wiesendanger, Science **341**, 636 (2013).

<sup>23</sup>Romming, N., A. Kubetzka, C. Hanneken, K. von Bergmann, and R. Wiesendanger, Phys. Rev. Lett. **114**, 177203 (2015).

<sup>24</sup>A. Derras-Chouk, E. M. Chudnovsky, and D. A. Garanin, Phys. Rev. B **98**, 024423-(9) (2018).

<sup>25</sup>D. Cortes-Ortuno, W. Wang, M. Beg, R. A. Pepper, M. Bisotti, and R. Carey, Sci. Rep. **7**, 4060 (2017).

<sup>26</sup>P. F. Bessarab, G. P. Müller, I. S. Lobanov, F. N. Rybakov, N. S. Kiselev, H. Jansson, V. M. Uzdin, S. Blugel, L. Bergqvist, and A. Delin, Sci. Rep. **8**, 3433 (2018).

<sup>27</sup>D. Stosic, J. Mulkers, B. Van Waeyenberge, T. B. Ludermir, and M. V. Milosevic, Phys. Rev. B **95**, 214418 (2017).

<sup>28</sup>L. Desplat, D. Suess, J.-V. Kim, and R. L. Stamps, Phys. Rev. B **98**, 134407 (2018).

<sup>29</sup>J. Hagemester, N. Romming, K. von Bergmann, E. Y. Vedmedenko, and R. Wiesendanger, Nat. Commun. **6**, 8455 (2015).

<sup>30</sup>S. Rohart, J. Miltat, and A. Thiaville, Phys. Rev. B **93**, 214412 (2016).

<sup>31</sup>L. Rozsa, E. Simon, K. Palotás, L. Udvardi, and L. Szunyogh, Phys. Rev. B **93**, 024417 (2016).

<sup>32</sup>A. S. Varentsova, M. N. Potkina, S. von Malottki, S. Heinze, P. F. Bessarab, Nanosystems: Phys. Chem. Math. **9**(3), (2018).

<sup>33</sup>A. Siemens, Y. Zhang, J. Hagemester, E. Y. Vedmedenko, and R. Wiesendanger et al 2016 New J. Phys. **18** 045021 (2016).

<sup>34</sup>W. Koshibae, N. Nagaosa, Sci. Rep. **7**, 42645 (2017).

<sup>35</sup>S. von Malottki, B. Dupé, P.F. Bessarab, A. Delin, and S. Heinze, Sci. Rep. **7**, 12299 (2017).

<sup>36</sup>L. D. Landau and E. M. Lifshitz, Z. Phys. Sowjet. **8**, 153 (1935).

<sup>37</sup>H. A. Kramers, Physica, **7**, 284 (1940).

<sup>38</sup>W. F. Brown, Jr., Phys. Rev., **130**, 1677 (1963).

<sup>39</sup>H. Braun, Journal of Applied Physics **76**, 6310 (1994).

<sup>40</sup>W. T. Coffey and Yu. P. Kalmykov, *The Langevin Equation*, 4th ed. Singapore: World Scientific, 2017.

<sup>41</sup>D. J. Byrne, W. T. Coffey, Yu. P. Kalmykov, and S. V. Titov, Physica A **527**, 121195 (2019).

<sup>42</sup>R. F. L. Evans, in *Handbook of Materials Modeling*, eds. W. Andreoni and S. Yip, Springer, 2018.

<sup>43</sup>D. A. Garanin, Phys. Rev. E **95**, 013306 (2017).

<sup>44</sup>D. A. Garanin, Phys. Rev. B **98**, 144425 (2018).

<sup>45</sup>J. Wild, T. N. G. Meier, S. Pöllath, M. Kronseider, A. Bauer, A. Chacon, M. Halder, M. Schowalter, A. Rosenauer, J. Zweck, J. Möller, A. Rosch, C. Pfeleiderer, C. H. Back, Sci. Adv. **3**, e1701704 (2017).

<sup>46</sup>O. A. Tretiakov and K. A. Matveev, Phys. Rev. B **71**, 165326 (2005).

<sup>47</sup>O. A. Tretiakov, T. Gramespacher, and K. A. Matveev, Phys. Rev. B **67**, 073303 (2003).